symmetry

MDPI

Article

Recognition Algorithm of Transient Overvoltage Characteristic Based on Symmetrical Components Estimation

Yanzan Han * and Jimeng Zhang

Department of Mechanical and Electrical, Henan Polytechnic Institute, Nanyang 473000, China; zhangjimeng10010@sina.com

* Correspondence: hanyanzan@163.com

Received: 11 November 2019; Accepted: 25 December 2019; Published: 7 January 2020

Abstract: The recognition of transient overvoltage characteristics is the premise of disturbance compensation of the transient overvoltage. Based on that, the recognition algorithm of transient overvoltage characteristics based on symmetrical components estimation was proposed. The generation mechanism of the transient overvoltage in gas insulated switchgear (GIS) was analyzed. Then, the transient overvoltage was measured via the capacitive sensor method. The three-phase voltage of ultra-high voltage grid was asymmetrical when the transient overvoltage appeared. At present, the asymmetrical three-phase voltage was decomposed into the superposition of a symmetrical positive-sequence component, a negative-sequence component, and a zero-sequence component via the symmetrical components estimation to build the superposition model. The model was decomposed via the trigonometric identity and the modified neural network of the least mean square learning rule was used to estimate the parameter vector of the characteristic quantity of the transient overvoltage in real time. The feasibility of the proposed algorithm was verified via comparing the simulation of the proposed algorithm and the algorithm based on dp transformation. The experimental results show that the proposed algorithm has the advantages of a small operand, high detection precision, and fast action.

Keywords: symmetrical components estimation; transient overvoltage; characteristic; recognition; components superposition; trigonometric identity

1. Introduction

The gas insulated switchgear (GIS) has the advantages of a compact structure, less land occupation, and easy maintenance [1]. Therefore, it is widely applied in the 110 kV or above power grid. All ultra-high voltage (UHV) AC transmission systems of China have adopted the GIS. In the GIS substation, the operation of the breaker, disconnecting switch, and earth switch and the short trouble of single-phase earth will generate the very fast transient overvoltage [2,3], of which the operation of disconnecting switch is the primary cause. The transient overvoltage has thr characteristics of high amplitude, steep wave front, high frequency, and multiple continuous pulses, which have great effects on the insulation of the GIS and the connected winding equipment (e.g., transformer). Meanwhile, the transient overvoltage will generate the transient enclosure voltage (TEV) at the joint of the GIS shell and theouter lead, causing the problem of safety and secondary equipment insulation and the forming of the electromagnetic interference to the measurement and control equipment, which generates the malfunction of the secondary equipment [4,5]. Therefore, the transient overvoltage has become the focus of researchers.

Aiming at the product design of GIS, some foreign manufacturers have researched the transient overvoltage generated by the disconnecting switch operation in the extra high voltage system since

the1980s. The measuring system of the transient overvoltage was designed. The characteristics, effect on equipment insulation, and electromagnetic interference on the secondary equipment of the transient overvoltage were analyzed via a simulation test and a digital simulation method [6,7]. Meanwhile, the method of the disconnecting switch installed with the damping resistance to suppress the transient overvoltage was proposed. Domestic researchers have simulated and calculated the transient overvoltage of the substation with 500 kV and 750 kV respectively, and carried out an actual measurement for the transmission project debugging with 750 kV. Seldom, foreign researchers focus on the transient overvoltage in the 1000 kV system and only Japanese researchers have researched that in extra high GIS [8], while China has carried out the simulating calculation of the transient overvoltage for the experiment and demonstration project of the UHV AC. The State Grid Corporation of China set up the project of actual measurement and simulation research on the transient overvoltage in the UHV GIS/HGIS equipment in 2009. Research on the measurement and simulation of transient overvoltage in the UHV system, insulation characteristic under overvoltage, TEV, and electromagnetic interference has been conducted. The staged progress has been obtained. Ma, Guo Ming et al. studied the time and frequency characteristics of transient overvoltage in ultra-high voltage substations with the use of a port hole sensor of the surface-mounted device to detect the on-site VFTO characteristics and obtain different levels of voltage steepness and the duration of frequency components. Under electromagnetic interference, transient overvoltage characteristics can be accurately identified, but this method requires too much calculation and takes too long to recognize. Hu, Jiabing et al. propose a DC voltage fault analysis and enhanced control method for HMC transmission system based on hybrid MMC. By analyzing the characteristics of pole-to-earth faults, an enhanced control strategy is proposed, and a new variable is allocated to distribute the power transmitted from the AC side, effectively eliminating overvoltage faults, and accurately identifying transient overvoltage characteristics. This method has short recognition time and is fast, but there are certain errors.

The compensation of transient overvoltage disturbance is achieved via various ways. The dynamic voltage restorer (DVR) has been identified as the most effective compensation device to solve the transient overvoltage [9]. The DVR requests fast response speed, hence fast and precise recognition on the transient overvoltage is the premise to apply the DVR rapidly into the compensation, which is a key technique that must be solved during the DVR research. At present, the most applied recognition algorithm is based on the normal and modified dp transformation [10]. However, both of them require a low pass filter to remove the transformed high-frequency component to solve effective value of the transient overvoltage and phase jump. Although various advanced filters are used during the design of a low pass filter, such as amathematical morphological filter, the response speed still decreases [11,12]. Moreover, the property of the method decreased drastically in the condition of voltage waveform distortion. The normal and modified Kalman filters have also been applied to the recognition on transient overvoltage, but are limited in the actual application because of the operation load and prior knowledge of noise required by the algorithm [13–15].

Therefore, this paper proposes a transient overvoltage characteristic recognition algorithm based on symmetric component estimation. This paper analyzes the transient overvoltage generation mechanism through GIS, measures the transient overvoltage value according to the capacitance sensor method, and estimates the transient three-phase phasor symmetrical component. In addition, we determine the transient overvoltage RMS value and phase transition to complete the transient overvoltage characteristic identification. Through the extraction experiments of the symmetrical components, the identification experiment of the transient overvoltage positive sequence component RMS value and the phase transition characteristics, and the identification effect experiments, the proposed algorithm is verified.

2. Definition of the Algorithm

Based on the analysis of the transient overvoltage generation mechanism, an electromagnetic interference control method is given. Based on this, a three-phase voltage decomposition model is

established, and the measured vector of the three-phase voltage is obtained through triangular identity decomposition to complete the identification of transient voltage characteristics. The specific process is shown in Figure 1.

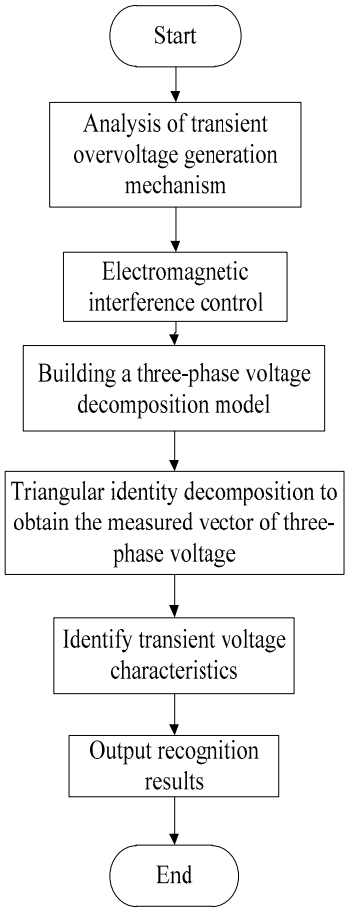

Figure 1. Algorithm implementation process.

2.1. Generation Mechanism of Transient Overvoltage

Multiple re-strikes were formed at the fracture interval of the disconnecting switch due to the slow kinematic velocity of contact when the short bus is no-load caused by the disconnecting switch operation in the GIS. The sharply changed traveling wave is generated. Then the wave is refracted, reflected, and superimposed in the node with wave impedance variation in GIS. Thus, the transient overvoltage is formed.

Figure 2 shows the mechanism of transient overvoltage generated by opening of the disconnecting switch. In the diagram, the U_s is the value of supply voltage and the U_1 is the value of residual voltage. The U_p represents the amplitude value of the transient overvoltage. Under the most serious condition that the contact space of disconnecting switch is broken down when both the U_s and U_1 are 1.0 pu, the maximum of U_p obtained via theoretical calculation is approximate or over 3.0 pu. Results of simulation and experiment show that the range of amplitude value of the transient overvoltage is from 1.5 pu to 2.8 pu [16]. The rise time of transient overvoltage is short, even as short as a few nanoseconds. The range of main frequency is from a few MHz to scores of MHz and the maximum frequency is 100 MHz. The re-strike times occurred in operation of the disconnecting switch depend on the speed of operation [17]. If the speed is fast, the times are less. Otherwise, the times are more. Generally, the number of re-strike is from tens to dozens of times.

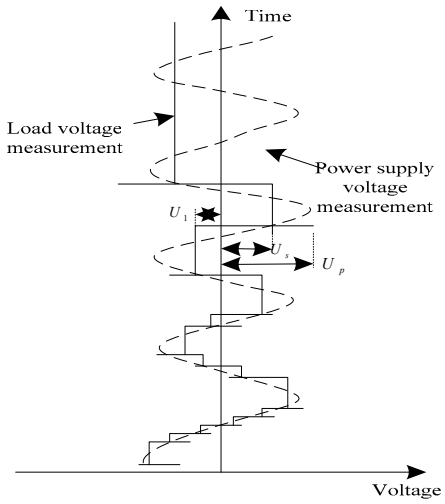

Figure 2. Schematic diagram of transient overvoltage generation mechanism.

Steep wavefront overvoltage generated between the high voltage conductors (stick) and shell is called interior transient overvoltage during the disconnecting switch operation in the GIS [18]. TEV and electromagnetic interference are generated outside the GIS shell due to the refraction and reflection of the voltage wave at the joint (nodes) between the shell and cable (or overhead) line during the diffusion of the wave, which is collectively known as the external transient overvoltage [19]. The interior transient overvoltage has significant effects on the GIS and the winding equipment connected with the GIS, while the external transient overvoltage transient overvoltage is harmful to the insulation of the secondary equipment connected with the shell, or causes electromagnetic interference to the secondary equipment. The transient voltage generation mechanism is obtained, which can effectively control electromagnetic interference, and then perform transient voltage measurements.

2.2. Measuring Method of Transient Overvoltage

According to the transient overvoltage generation mechanism in the previous section, the cause of the measurement error is analyzed, and the transient voltage measurement can be implemented in a targeted manner. The transient overvoltage is measured via experiment because of its complex phenomenon and strong randomness. To recognize the characteristic accurately, research on measuring methods is necessary.

The research on measuring methods for transient overvoltage has been carried out early by Canada, Japan, Germany, and Switzerland. The measuring systems with capacitive sensors with hand-hole type and pre-embedded ring type and electric field probes have been developed and applied to the laboratory test and field measurement. China developed the capacitive sensors with hand-hole type in the 1990s applied to measurement for transient overvoltage in 252 kV test loop. At the beginning of the 21st century, a preliminary exploration of the capacitive sensors with pre-embedded ring type was conducted. The measurement method of bushing tap of transformer and high voltage parallel reactor was proposed and applied to the measurement for the transient overvoltage in the 750 kV project debugging. Figure 3 shows the measurement principle of capacitance sensor method.

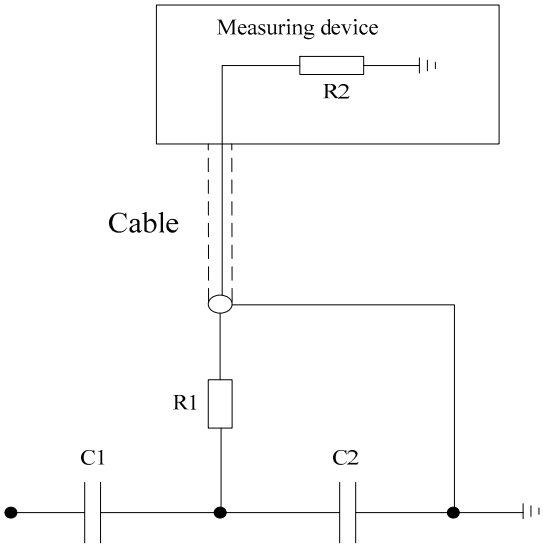

Figure 3. Measurement principle of capacitance sensor method.

The capacitance is composed of C1 and C2. The R1 is the matched resistance of the cable. The measurement device includes an oscilloscope, a buffer amplifier and trigger circuit, a sensor, matched resistance, a cable, and measuring equipment, which together constitute the measurement system [20–23]. The signal obtained by the capacitance sensor is input to the measuring equipment via the cable for the collection and storage. The frequency response characteristics of the measurement system of capacitance sensor are related to the input impedance R2 of the measuring equipment, which needs the suitable designed R2 to acquire the frequency range of the measurement of transient overvoltage.

The capacitance sensor has two structural styles, the hand-hole type and the pre-embedded ring type, as shown in Figure 4. The plate electrode is installed via trepanning on the GIS shell in the hand hole-type capacitance sensor. The high voltage arm is the capacitance C1 consisting of the plate electrode and GIS high-voltage guide rod, while the low-voltage arm is the external capacitance C2 or the capacitance consisting of the plate electrode and shell. The pre-embedded ring-type capacitance sensor includes capacitance C1 consisting of internally shielded electrode embedded in basin-type insulator beforehand and high-voltage guide rod and external capacitance C2. In Figure 4b, the CL and LL are the external circuits.

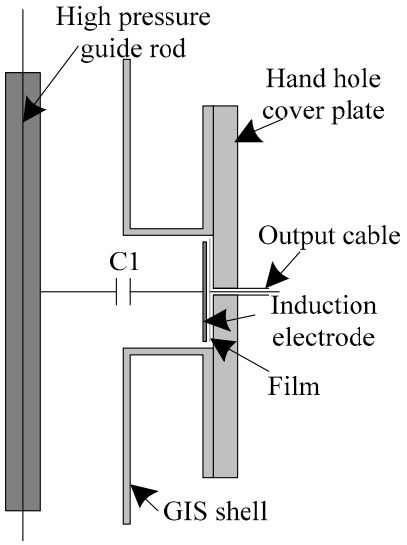

(**a**) the hand-hole type

Figure 4. *Cont.*

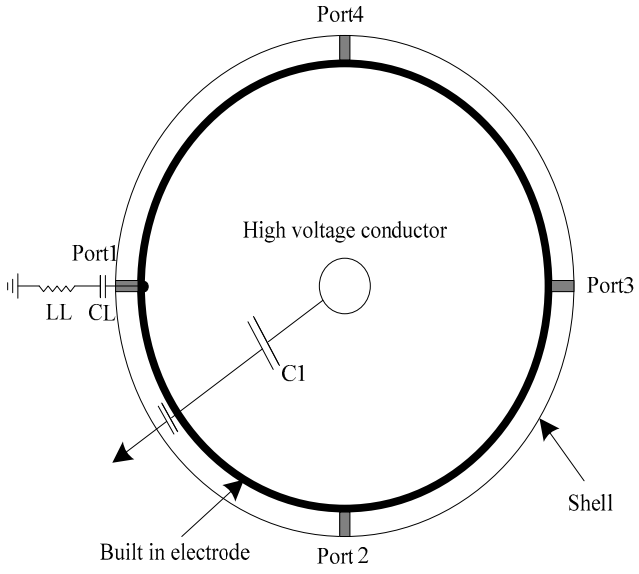

(**b**) the pre-embedded ring type

Figure 4. Capacitance sensor type.

The precise transient overvoltage is acquired via the capacitance sensor method. The characteristic of transient overvoltage is identified via the method of symmetrical components estimation after the transient overvoltage appears.

2.3. Symmetrical Components Estimation of Three-Phase Vector of Transient Overvoltage

The three-phase voltage of the ultra high-voltage grid is in an asymmetrical state when the transient overvoltage appears. Now, the asymmetrical three-phase voltage can be decomposed into the superposition of symmetrical positive-sequence component, negative-sequence component, and zero-sequence component. The superposition model is shown in Formula (1). The superposition model is the basis of the proposed algorithm.

$$\begin{pmatrix} v_a \\ v_b \\ v_c \end{pmatrix} = V_0 \begin{pmatrix} \sin(wt+\varphi_0) \\ \sin(wt+\varphi_0) \\ \sin(wt+\varphi_0) \end{pmatrix} + V_+ \begin{pmatrix} \sin(wt+\varphi_+) \\ \sin(wt+\varphi_+ - 120^\circ) \\ \sin(wt+\varphi_+ + 120^\circ) \end{pmatrix} + V_- \begin{pmatrix} \sin(wt+\varphi_-) \\ \sin(wt+\varphi_- + 120^\circ) \\ \sin(wt+\varphi_- - 120^\circ) \end{pmatrix} \quad (1)$$

Equation (1) represents an asymmetric three-phase voltage decomposition model, which is obtained by superposing a positive sequence component, a negative sequence component, and a zero sequence component, respectively. Among the Formula (1), v_a, v_b and v_c is the three-phase voltage in the gird during the generation of transient overvoltage. V_0 and φ_0 represent the amplitude value and phase position of the zero-sequence symmetrical component respectively. V_+ and φ_+ represent the amplitude value and phase position of the positive-sequence symmetrical component respectively. V_- and φ_- represent the amplitude value and phase position of the negative-sequence symmetrical component respectively. The decomposition is carried out via the trigonometric identity as shown in Formula (2):

$$\sin(\alpha+\beta) = \sin\alpha\cos\beta + \cos\alpha\sin\beta \quad (2)$$

The decomposed superposition model for Formula (1) is obtained via Formula (2), as shown in Formula (3):

$$\begin{aligned}\begin{pmatrix} v_a \\ v_b \\ v_c \end{pmatrix} &= V_0 \begin{pmatrix} \sin(wt)\cos\phi_0 + \cos(wt)\sin\phi_0 \\ \sin(wt)\cos\phi_0 + \cos(wt)\sin\phi_0 \\ \sin(wt)\cos\phi_0 + \cos(wt)\sin\phi_0 \end{pmatrix} \\ &+ V_+ \begin{pmatrix} \sin(wt)\cos\phi_+ + \cos(wt)\sin\phi_+ \\ \sin(wt-120^\circ)\cos\phi_+ + \cos(wt-120^\circ)\sin\phi_+ \\ \sin(wt+120^\circ)\cos\phi_+ + \cos(wt+120^\circ)\sin\phi_+ \end{pmatrix} \\ &+ V_- \begin{pmatrix} \sin(wt)\cos\phi_- + \cos(wt)\sin\phi_- \\ \sin(wt+120^\circ)\cos\phi_+ + \cos(wt+120^\circ)\sin\phi_+ \\ \sin(wt-120^\circ)\cos\phi_+ + \cos(wt-120^\circ)\sin\phi_+ \end{pmatrix}\end{aligned} \tag{3}$$

Supposing $v(t) = \begin{pmatrix} v_a \\ v_b \\ v_c \end{pmatrix}$, $W = \begin{pmatrix} V_0\cos\phi_0 \\ V_0\sin\phi_0 \\ V_+\cos\phi_+ \\ V_+\sin\phi_+ \\ V_-\cos\phi_- \\ V_-\sin\phi_- \end{pmatrix}$, $X(t) = \begin{pmatrix} \sin(wt) & \sin(wt) & \sin(wt) \\ \cos(wt) & \cos(wt) & \cos(wt) \\ \sin(wt) & \sin(wt-120^\circ) & \sin(wt+120^\circ) \\ \cos(wt) & \cos(wt-120^\circ) & \cos(wt+120^\circ) \\ \sin(wt) & \sin(wt+120^\circ) & \sin(wt-120^\circ) \\ \cos(wt) & \cos(wt+120^\circ) & \cos(wt-120^\circ) \end{pmatrix}$, matrix form as shown in Formula (4) can be obtained:

$$v(t) = X(t)^T W \tag{4}$$

In the Formula (4), the $v(t)$ represents the real-time measurement vector of the tree-phase voltage in grid when the transient overvoltage appears. The $X(t)$ represents vector of time-varying matrix coefficient. The W is parameter vector waiting for estimation containing characteristics quantity of the transient overvoltage.

2.4. Confirmation of Effective Value and Phase Jump of Transient Overvoltage

According to the need for simultaneous detection of three-phase voltages in the power grid, an improved minimum mean square learning rule neural network is used to estimate the transient overvoltage characteristic parameter parameter vector N_N. $W(3) = V_+\cos\phi_+$. $W(4) = V_+\sin\phi_+$. Therefore, the effective value and phase position of the positive sequence are shown in the Formulas (5) and (6).

$$N_N = V_+ / \sqrt{2} = \sqrt{\frac{W(3)\text{^}2 + W(4)\text{^}2}{2}} \tag{5}$$

$$\theta = \arctan\frac{W(4)}{W(3)} \tag{6}$$

According to Formulas (5) and (6), the characteristic can be operated and recognized immediately without any extra operation.

3. Experimental Analysis

3.1. Analysis on Extraction Ability of Symmetrical Components

The three-phase voltage in the grid is decomposed into the superposition of positive-sequence component, negative-sequence component, and zero-sequence component under the condition of transient overvoltage. According to the proposed algorithm, the waveform of decomposition process of the symmetrical components is shown in Figure 5.

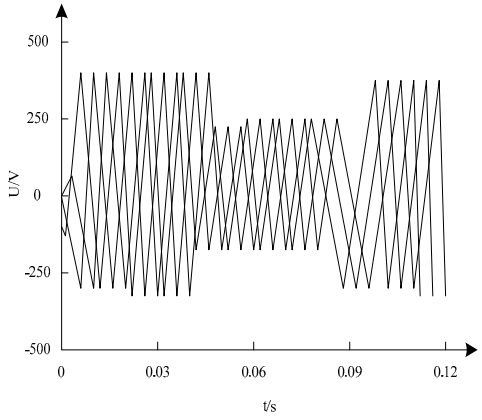

(**a**) positive sequence component

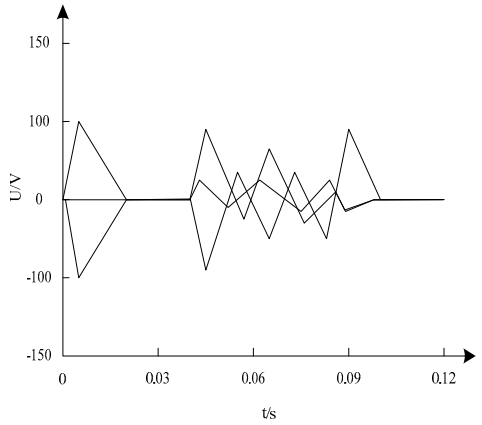

(**b**) negative sequence component

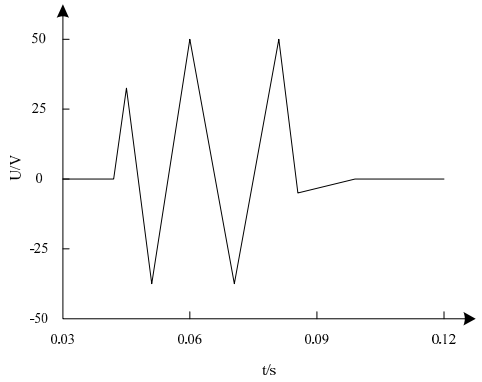

(**c**) zero sequence component

Figure 5. Process curve of symmetric component estimation.

It can be seen from Figure 5 that the proposed algorithm can decompose the three-phase voltage into a positive-sequence component, negative-sequence component, and a zero-sequence component rapidly and precisely after transient overvoltage. It can provide the basis for the characteristic recognition of the transient overvoltage and subsequent compensation control.

3.2. Characteristic Recognition on Effective Value and Phase Jump of Positive-Sequence of Transient Overvoltage

To identify the validity, the proposed algorithm is compared with the recognition algorithm based on the dq transformation method. Because of the 100 Hz signal of the negative-sequence component generated after the dp transformation, the Butterworth digital low pass filter with four orders and 60 Hz cut-off frequency is chosen after weighing the delay time and filter effect in the algorithm based on the dp transformation. To compare the property of two recognition algorithms, index parameters are defined as follows:

(1) Actuation time t_1. It is the time that effective value curve of the detected positive-sequence component crossing the 90% normal voltage fundamental wave takes from the moment when the transient overvoltage occurs or ends.
(2) Adjustment time t_2. It is the time that effective value curve of the positive-sequence component entering and maintaining within ±3% error range of effective value of actual positive sequence component takes from the moment when the transient overvoltage occurs or ends.
(3) Effective value precision σ_1. It is the maximum deviation between the detected fundamental wave effective value and the actual fundamental wave effective value after the transient overvoltage is stable experiencing the adjustment time t_2 test, which is represented as percentage of the actual fundamental wave effective value.
(4) Phase position precision σ_2. It is the maximum deviation between the detected fundamental wave phase position and the actual fundamental wave phase position after the transient overvoltage is stable experiencing the adjustment time t_2 test, which is represented as percentage of the actual phase jump.

The following experimental verification is used. This paper uses EMTP software to identify the transient overvoltage characteristics during the start and recovery of the sag. Among them, the filter voltage is 12 V, the current is 30 A, the sum of the arcing coil loss resistance and damping resistance is set to 200 Ω, the inductive reactance is 10 Ω, and the power factor is 0.8. Based on this, the transient overvoltage characteristic detection experiment is completed.

The effective value and phase position waveform of the detected positive-sequence component during the starting and recovering process are shown in Figures 6 and 7, respectively. Table 1 compared the index parameters of the two algorithms during the starting and recovering process.

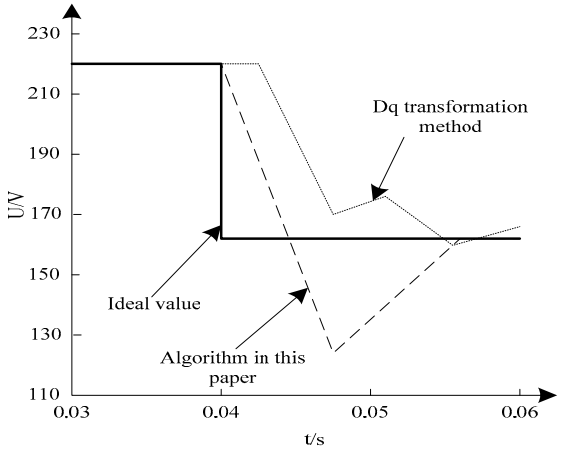

(**a**) starting process of transient overvoltage

Figure 6. *Cont.*

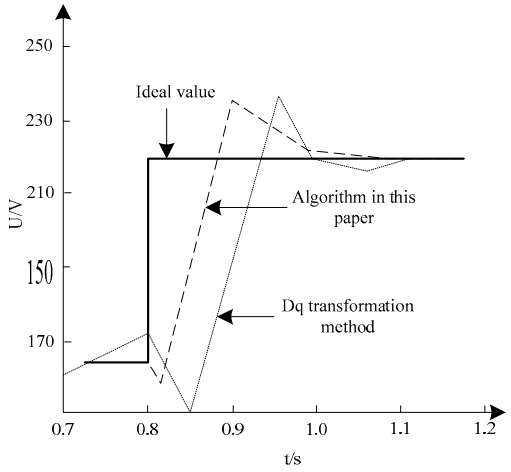

(**b**) transient overvoltage recovery process

Figure 6. Detected positive sequence component effective value.

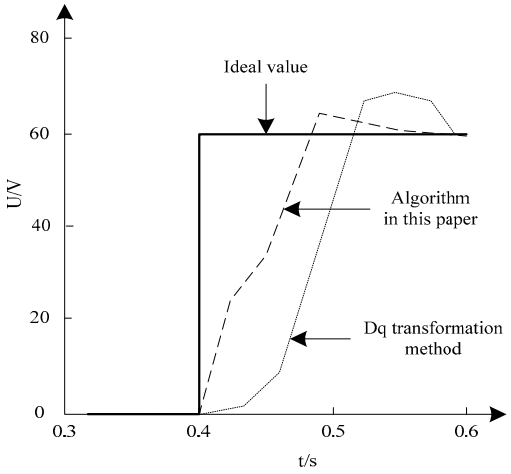

(**a**) starting process of transient overvoltage

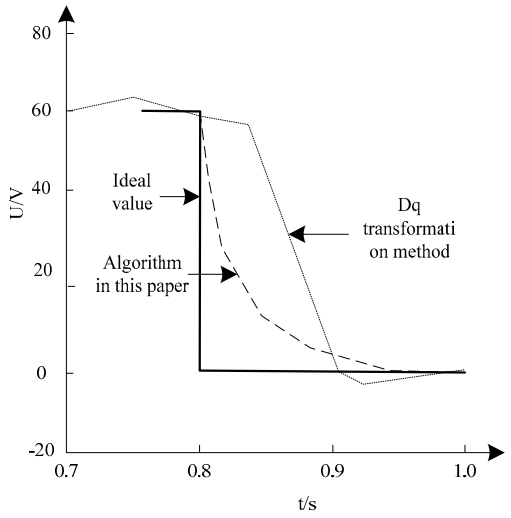

(**b**) transient overvoltage recovery process

Figure 7. Detected phase jump of positive sequence component.

Table 1. Comparison of recognition results.

Recognition Algorithm		Algorithm in This Paper	Dq Transform Algorithm
Starting process of transient overvoltage	t_1/ms	1.19	5.02
	t_2/ms	14.19	13.01
Transient overvoltage recovery process	t_1/ms	5.38	10.19
	t_2/ms	14.57	20.79
σ_1		Less than 1	3.58
σ_2		Less than 1	11.88

It can be seen from the Figures 6 and 7 and Table 1 that both the amplitude value and phase position detection of the proposed algorithm start to act with hardly any delay when the transient overvoltage occurs. While the normal algorithm with low pass filter based on the dq transformation inevitably has some delay. The proposed algorithm is almost zero steady state error during the characteristic recognition, while the error of the normal algorithm is fluctuant because of the restriction of filter design. To improve the detection precision, the only way is to increase the order of filter or reduce the cut-off frequency, which brings out increase of response time inevitably.

As shown in Figure 6, because of the too fast rate of descent, the proposed algorithm shows larger overshoot when it becomes stable during the transient overvoltage begins. It rises the adjustment time, which is the undesirable. Thus, the algorithm needs further improvement. It can be seen from Table 1 that the proposed algorithm has advantages in detection of effective value, speed of phase variation and precision compared with the algorithm based on the dq transformation.

3.3. Recognition of Waveform Characteristics of Transient Overvoltage

The waveform characteristics, including peak value, wavefront time, steepness, frequency, and the number of re-strike are obtained via the statistic analysis using the proposed algorithm. The probability distribution of maximum transient overvoltage without pre-charging DC voltage of the rapid and slow disconnecting switch is shown in Figure 8.

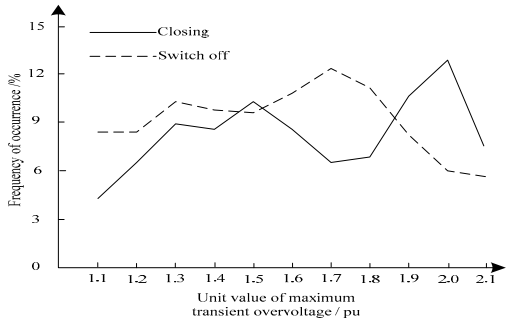

(**a**) quick disconnector

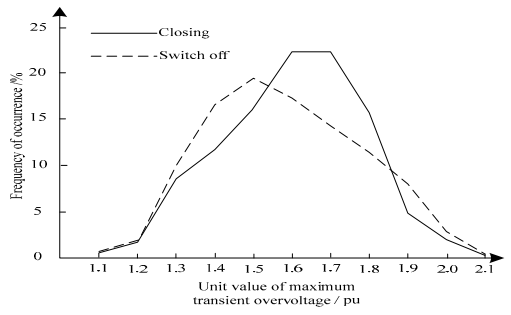

(**b**) slow speed disconnector

Figure 8. Probability distribution of maximum transient overvoltage without pre-charging DC voltage.

As shown in Figure 8, the maximum of transient overvoltage is 2.24 pu. The major frequency range is 6–8 MHz and the maximum frequency is 60 MHz, respectively. It is shown that the disconnecting switch with damping resistance can reduce the maximum of transient overvoltage to 2.24 pu.

In order to further verify the recognition effect of this method, the accuracy of voltage recognition under different methods is tested, and the results are shown in Figure 9.

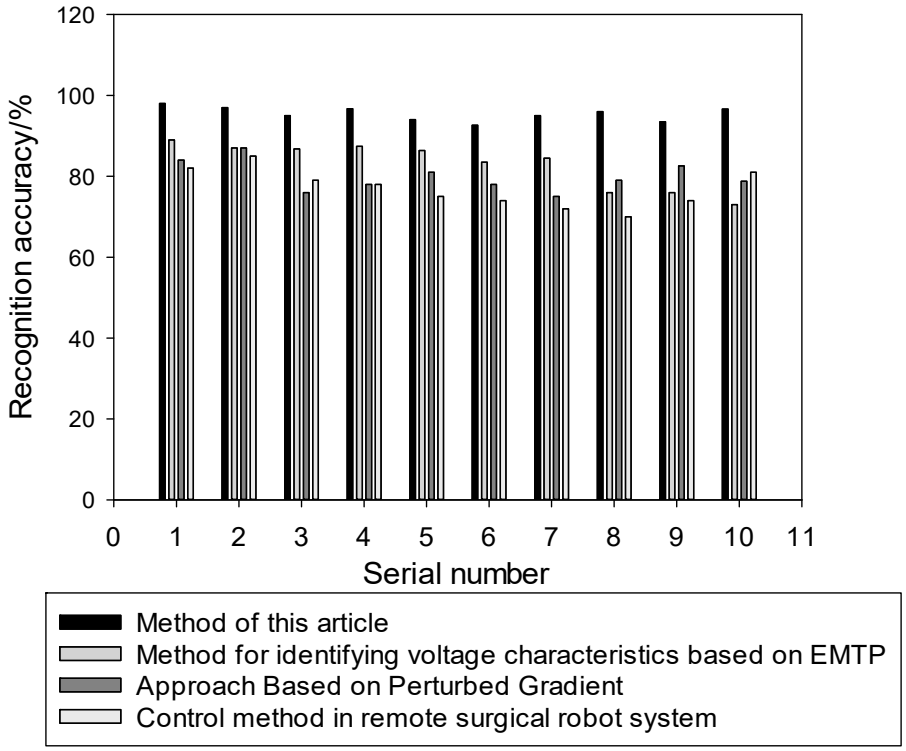

Figure 9. Accuracy of voltage identification under different methods.

According to Figure 9, different methods have different voltage recognition accuracy, and they are all above 70%.Taking the group 4 experiment as an example, the recognition accuracy of the method in this paper is 96%.The recognition accuracy of the method for identifying voltage characteristics based on EMTP is 87.4%.The recognition accuracy of the approach based on perturbed gradient is 78%. The recognition accuracy of the control method in remote surgical robot system is 78%. The other three methods are obviously not as accurate as the method in this paper, which indicates the voltage identification characteristics of the method in this paper.

4. Discussion

Comparing the convergence of different methods; the results are shown in Figure 10.

The analysis of the above figure shows that the convergence of different methods is different. Compared other important methods, this method has the best convergence.

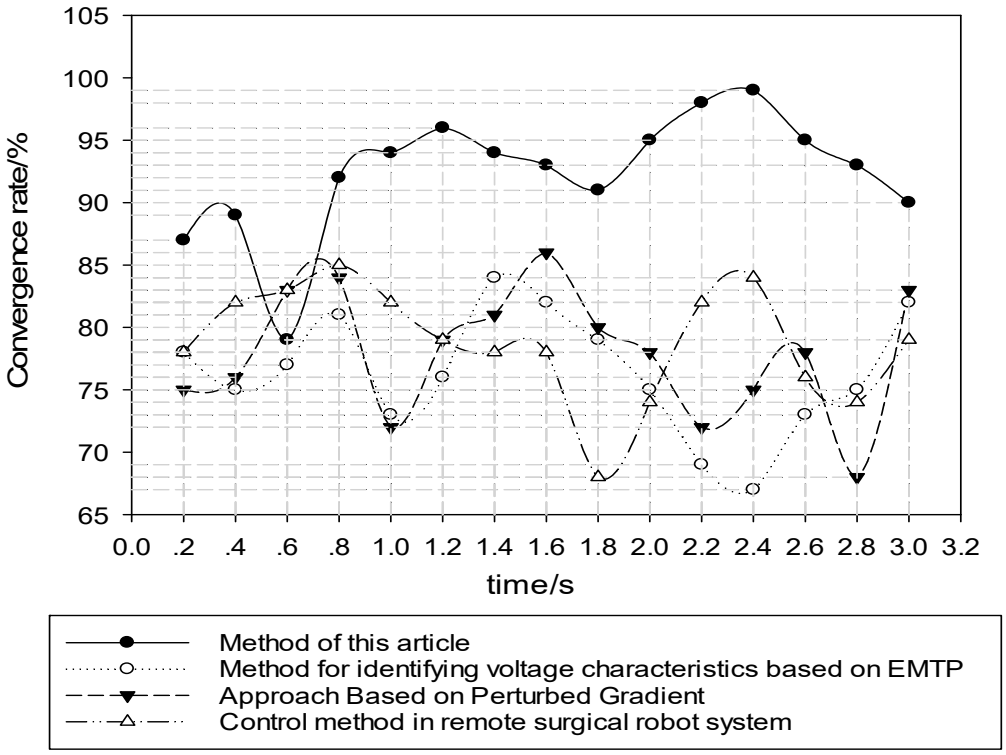

Figure 10. Convergence of different methods.

With the vigorous development of national economy, the electric power industry has been reformed and perfected, and has become more modern. Currently, a very fast transient phenomenon generated by the disconnecting switch operation in the GIS has received extensive attention from researchers, in which the overvoltage is called as very fast transient overvoltage with the most important characteristics of high amplitude and steep wave front. Therefore, it causes threats towards the equipment insulation, especially for the extra-high voltage equipment. At present, the experimental investigation on transient overvoltage in the extra-high voltage GIS is still scarce due to the restriction of test conditions and measuring means around the world. Hence, to satisfy the requirement of design and operation of extra-high voltage projects and equipment in China, it is necessary to carry out large-scale experimental studies for the characteristic of transient overvoltage in the extra-high voltage GIS. For that purpose, the State Grid Corporation of China set up the project of actual measurement and simulation research on the transient overvoltage in the UHV GIS/HGIS equipment in 2009. The test loop of transient overvoltage in the extra-high voltage GIS was built in the base of extra-high voltage AC test in Wuhan and the large-scale experimental study was carried out. Several beneficial results were obtained. On that basis, the recognition algorithm of transient overvoltage characteristic based on symmetrical components estimation is proposed in this article. The transient overvoltage is further measured and the characteristic of the transient overvoltage is recognized via the symmetrical components estimation.

Signals of electrical power systems are almost three-phase sinusoidal signals. When the value of amplitude of a group of the three-phase sinusoidal signal is equal and the phase difference is 120°, the three-phase electrical power system is balanced. Otherwise, the system is unbalanced. The symmetrical components theory considers that the signal of asymmetrical three-phase electrical power system can be decomposed into three signals with positive sequence, negative sequence, and zero sequence. When the power system operates in the known frequency state, the signals with positive sequence, negative sequence, and zero sequence only depend on their amplitude value and phase. Thus, the operation state of the power system depends on the amplitude value and phase of the three signals. Therefore, the symmetrical components theory becomes an important tool to analyze the transient overvoltage of the three-phase extra-high voltage electrical power system. At present, the symmetrical

components theory has been widely applied in the digital protection, harmonic governance, and fault analysis of the power system element.

The algorithm proposed in this article is deduced in detail via the theoretical formula. It is applied to the actual characteristic recognition of the transient overvoltage. The reliable recognition results are obtained via the simulation analysis. Meanwhile, the computation speed of the algorithm is fast and the memory occupation is small. However, compared with other algorithms, the time advantage of the algorithm has not been analyzed and compared in detail, which is suggested to be further studied in the future work.

5. Conclusions

To satisfy the requirement of real-time characteristic recognition, when the transient overvoltage appears in the ultra-high voltage grid, the generation mechanism is studied. The symmetrical components theory is used to build the symmetrical components model of the three-phase voltage in the gird. According to the requirement of simultaneous detection on the three-phase voltage, the parameter vector of characteristic quantity of the transient overvoltage is estimated in real time via the modified neural network of the least mean square learning rule. The principle of the algorithm is simple. The operand is small and detection precision is high. Therefore, the algorithm is suitable for the real-time detection. The simulation results show that the algorithm can satisfy the requirement of characteristic recognition well. Although the algorithm is verified via the simulation experiment, it still needs to be further verified in the next device development.

Author Contributions: This paper studies the transient overvoltage characteristics identification based on symmetric component estimation, analyzes the transient overvoltage generation mechanism in GIS, and uses the capacitive sensor method to measure the transient overvoltage. When transient overvoltage occurs, the three-phase voltage of the UHV grid is in an asymmetric state. At this time, the symmetrical component estimation method is used to decompose it into symmetrical positive sequence components, negative sequence components, and zero sequence components to construct a superposition model. Real-time estimation of characteristic vector of transient overvoltage characteristic parameters using improved minimum mean method. The method in this paper has the advantages of small calculation amount, high detection accuracy and high efficiency. Y.H. and J.Z. designed the methods and concepts of this article. Y.H. completed the experimental analysis section. Y.H. and J.Z. finished writing this article. All authors have read and agreed to the published version of the manuscript.

Funding: This research received no external funding.

Conflicts of Interest: No conflict of interest exits in the submission of this manuscript, and manuscript is approved by all authors for publication. I would like to declare on behalf of my co-authors that the work described was original research that has not been published previously, and not under consideration for publication elsewhere, in whole or in part. All the authors listed have approved the manuscript that is enclosed.

References

1. Ma, G.M.; Li, C.R.; Li, X. Time and frequency characteristics of very fast transient overvoltage in ultra high voltage substation. *IEEE Trans. Dielectr. Electr. Insul.* **2017**, *24*, 2459–2468. [CrossRef]
2. Shi, W.W.; Yan, J.P. A novel digital phase-locked loop under three-phase unbalance voltages based on ellipse fitting method. *J. Power Supply* **2017**, *15*, 60–64.
3. Sima, W.; Rui, H.; Yang, Q. Dual $LiNbO_3$ Crystal-based batteryless and contactless optical transient overvoltage sensor for overhead transmission line and substation applications. *IEEE Trans. Ind. Electron.* **2017**, *64*, 7323–7332. [CrossRef]
4. Wu, H.T.; Xiang, C.; Liu, X.F. Characteristics of electromagnetic disturbance for intelligent component due to switching operations via a 1100 kV AC GIS test circuit. *IEEE Trans. Power Deliv.* **2017**, *32*, 2228–2237.
5. On the construction of multi-relational classifier based on canonical correlation analysis. *Int. J. Artif. Intell.* **2019**, *17*, 23–43.
6. Hu, J.; Xu, K.; Lei, L. Analysis and enhanced control of hybrid-MMC-based HVDC systems during asymmetrical DC voltage faults. *IEEE Trans. Power Deliv.* **2017**, *32*, 1394–1403.
7. Sadeghkhani, I.; Golshan, M.E.H.; Guerrero, J.M. A current limiting strategy to improve fault ride-through of inverter interfaced autonomous microgrids. *IEEE Trans. Smart Grid* **2017**, *8*, 2138–2148. [CrossRef]

8. Khawaja, A.H.; Qi, H. Estimating sag and wind-induced motion of overhead power lines with current and magnetic-flux density measurements. *IEEE Trans. Instrum. Meas.* **2017**, *66*, 897–909. [CrossRef]
9. Yang, X.Y.; Wen, Z.T.; Lu, X.H. Preparation of $LiNi_{0.5}Mn_{1.5}O_4$ as high-voltage cathode material and its rate capability. *Chin. J. Power Sources* **2017**, *41*, 345–347.
10. Naderi, S.B.; Negnevitsky, M.; Jalilian, A. Optimum resistive type fault current limiter: An efficient solution to achieve maximum fault ride-through capability of fixed-speed wind turbines during symmetrical and asymmetrical grid faults. *IEEE Trans. Ind. Appl.* **2017**, *53*, 538–548. [CrossRef]
11. Zhang, Z.Y.; Rui, H.R.; Liu, H.C.; Liu, Y.P. Simulation analysis of sheath overvoltage characteristic for single-phase ground fault in high voltage single-core cable. *Electr. Meas. Instrum.* **2018**, *55*, 115–119.
12. Awati, V.B.; Naik, S.; Mahesh, K.N. Multigrid method for the solution of EHL line contact with bio-based oils as lubricants. *Appl. Math. Nonlinear Sci.* **2016**, *1*, 359–368. [CrossRef]
13. Hasanien, H.M. Performance improvement of photovoltaic power systems using an optimal control strategy based on whale optimization algorithm. *Electr. Power Syst. Res.* **2018**, *157*, 168–176. [CrossRef]
14. Spall, J.C. Multivariate stochastic approximation using a simultaneous perturbation gradient approximation. *IEEE Trans. Autom. Control* **1992**, *37*, 332–341. [CrossRef]
15. Árpád, T.; Levente, K.; Imre, J.R.; Radu-Emil, P.; Tamás, H. Models for force control in telesurgical robot systems. *Acta Polytech. Hung.* **2015**, *12*, 95–114.
16. Lin, Y.; Liu, Y.; Li, G.M. An online monitoring method for capacitive voltage transformer based on SCADA system authors. *Autom. Instrum.* **2018**, *1*, 37–40.
17. Zhang, X.; Huaxing, L.I.; Huang, Y. Leading-edge flow separation control over an airfoil using a symmetrical dielectric barrier discharge plasma actuator. *Chin. J. Aeronaut.* **2019**, *32*, 137–150. [CrossRef]
18. Khawaja, A.H.; Qi, H.; Jian, L. Estimation of current and sag in overhead power transmission lines with optimized magnetic field sensor array placement. *IEEE Trans. Magn.* **2017**, *53*, 1–10. [CrossRef]
19. Sadeghkhani, I.; Golshan, M.E.H.; Mehrizi-Sani, A. Low-voltage ride-through of a droop-based three-phase four-wire grid-connected microgrid. *IET Gener. Transm. Distrib.* **2018**, *12*, 1906–1914. [CrossRef]
20. Martinez, M.I.; Susperregui, A.; Tapia, G. Second-order sliding-mode-based global control scheme for wind turbine-driven DFIGs subject to unbalanced and distorted grid voltage. *IET Electr. Power Appl.* **2017**, *11*, 1013–1022. [CrossRef]
21. Zhang, J.B.; Chen, Z.H.; He, C.Y. Identification of var-voltage characteristics based on ambient signals. *IEEE Trans. Power Syst.* **2018**, *33*, 3202–3203. [CrossRef]
22. Egorchev, M.; Tiumentsev, Y. Neural network identification of aircraft nonlinear aerodynamic characteristics. *IOP Conf. Ser. Mater. Sci. Eng.* **2018**, *312*. [CrossRef]
23. von Larcher, T.; Klein, R. On identification of self-similar characteristics using the Tensor Train decomposition method with application to channel turbulence flow. *Theor. Comput. Fluid Dyn.* **2019**, *33*, 141–159. [CrossRef]